31st EPS Conference on Plasma Phys. London, 28 June - 2 July 2004 ECA Vol.28G, P-4.190 (2004)

# Gyrokinetic Microstability Calculations for MAST

D Applegate[1], C M Roach, J W Connor, S C Cowley[1], W D Dorland[2], N Joiner[1],

R J Akers, N J Conway, A R Field, A Patel, M Valovic, M J Walsh[3] and the MAST team

*EURATOM/UKAEA Fusion Association, Culham Science Centre, Abingdon, Oxon, UK*

1. *Imperial College, London, UK*
2. *University of Maryland, US*
3. *Walsh Scientific Ltd., Culham Science Centre, Abingdon, Oxon, UK*

## Introduction

There is considerable interest in understanding the properties of microinstabilities and their impact on heat and particle confinement in tokamak plasmas, including in the novel tight aspect ratio spherical tokamak (ST) configuration. STs exhibit strong magnetic field variation, and achieve very high ratios of plasma pressure to magnetic field strength, β. Both of these factors are known to have important influences on microstability. Ion heat transport has been found to lie close to the neoclassical theory predictions in a number of STs [1-3], and the NSTX experiment has reported dominant heat transport losses occurring in the electron channel [3]. Gyrokinetic analyses of microstability for NSTX plasmas [4,5] have found that ion temperature gradient driven modes (ITG) are stabilised and electron temperature gradient driven modes (ETG) destabilised at the observed high ratios of $T_i/T_e$, which is consistent with the low levels of ion heat transport and high levels of electron heat transport in these discharges. It is of interest whether MAST will confirm this finding with increased auxiliary heating power. The study of microinstabilities could shed light on these phenomena, and on internal transport barriers which have also been observed in MAST [6].

## Microstability Calculations

This paper exploits the GS2 code [7] to perform gyrokinetic microstability analyses, both with and without electromagnetic (EM) effects, on three surfaces ($\psi_n$=0.4, 0.6 and 0.8) of a modest β MAST-like equilibrium, based on that from ELMy H-mode #6252 at t=0.265s, and illustrated in Figure1. Thomson scattering and spectroscopy measurements were used to prescribe the pressure profile and local profile

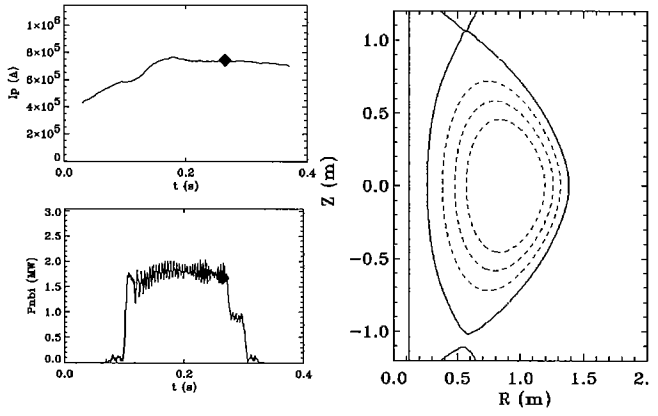


Figure1: Time traces of $I_p$ and $P_{nbi}$ and the reconstructed equilibrium at t=0.265s for ELMy H-mode MAST shot #6252.

derivatives, and the neutral beam fast ions were modelled using the LOCUST Monte Carlo code. Simple model assumptions were made to include two impurity species, C and O. GS2 is an initial value code, and has been used to find the fastest growing instabilities as a function of perpendicular wavenumber $k_y$, in two length-scale regimes: (i) $k_y\rho_i \leq O(1)$ (ITG) and (ii) $1/\rho_i < k_y \leq O(1/\rho_e)$ (ETG).

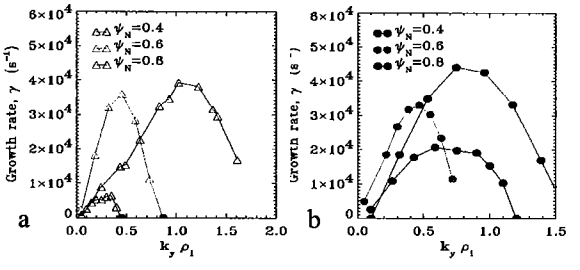


Figure2: Growth rates of dominant modes in (a) electrostatic and (b) electromagnetic calculations on all surfaces as functions of $k_y\rho_i$.

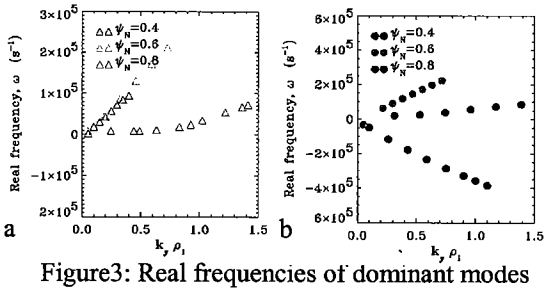


Figure3: Real frequencies of dominant modes in (a) electrostatic and (b) electromagnetic calculations on all surfaces as functions of $k_y\rho_i$.

In calculations with $k_y\rho_i \leq O(1)$ the linear gyrokinetic equation was solved for all five plasma species. Figures 2,3 give the growth rates, $\gamma$, and real frequencies, $\omega$, of the fastest growing modes. Electrostatic (ES) calculations found ITG character modes rotating in the ion diamagnetic direction and with $\omega \propto k_y$. While the impact of electromagnetic effects on the

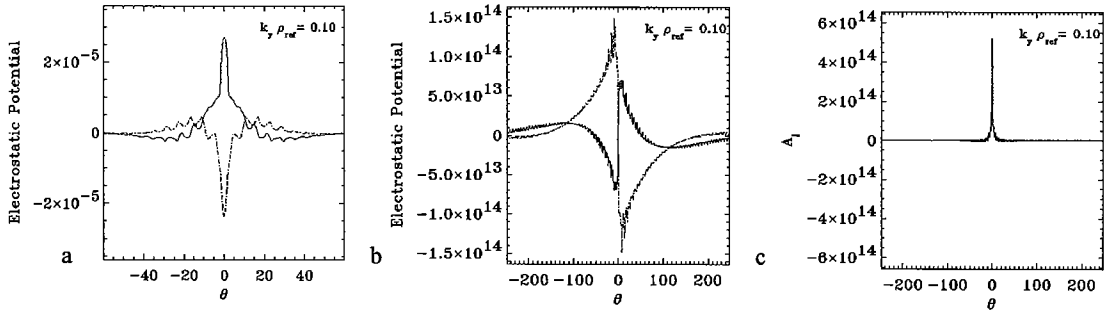


Figure4: Fastest growing eigenmodes at perpendicular wavenumber $k_y\rho_i = 0.1$ on surface $\psi_n = 0.4$ (a) $\Phi$ from an electrostatic calculation, (b) $\Phi$ and (c) $A_{||}$ from an electromagnetic calculation. Real and imaginary parts are represented by solid blue and dashed red lines respectively.

fastest growing modes was modest on the outer flux surfaces, it was dramatic on the inner surface where faster growing modes with markedly different character were found rotating in the electron diamagnetic drift direction. Figure 4 shows eigenfunctions of the electrostatic potential, $\Phi$, and the parallel magnetic vector potential, $A_{||}$ as functions of the ballooning angle $\theta$ for the fastest growing modes on the $\psi_n = 0.4$ surface, with $k_y\rho_i = 0.1$, in both electrostatic and electromagnetic calculations. All unstable electromagnetic modes on the surface $\psi_n = 0.4$ exhibit tearing parity (ie $A_{||}$ is even in $\theta$) and are extremely extended along the magnetic field (ie in $\theta$). Computing growth rates for the tearing parity modes is

extremely demanding, owing to the large number of points that are required in the θ grid. On removing electron collisions, the dominant mode growth rates are reduced and these modes revert to ITG drift wave character. Scans in $\eta_i$ (where $\eta_i = L_{ni} / L_{Ti}$) at constant pressure profile (simultaneously modifying $\eta_e$ to preserve quasi-neutrality away from the flux surface) have confirmed that the electrostatic ITG mode can be stabilised at low values of $\eta_i$. In shorter length scale calculations with $1/\rho_i < k_y \leq O(1/\rho_e)$ we have modelled the ions as a single species with an adiabatic response, and have solved the gyrokinetic equation only for the electron species. The ETG instabilities computed rotate in the electron diamagnetic drift direction and have much larger growth rates than the ITG instabilities. EM effects have little impact on the character of the fastest growing modes, but do stabilise modes on all surfaces, most significantly on the inner surface with highest β.

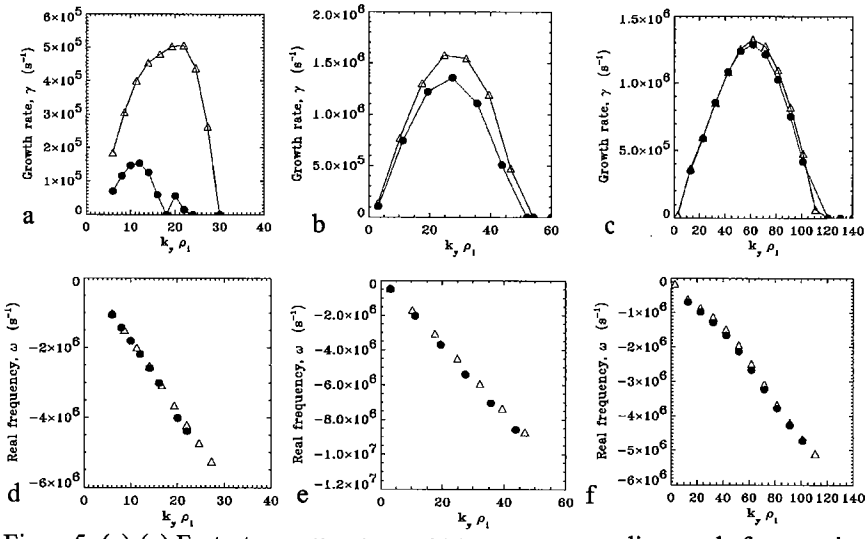


Figure5: (a)-(c) Fastest growth rates and (d)-(f) corresponding mode frequencies as function of $k_y\rho_i$ on surfaces $\psi_n$=0.4, 0.6 and 0.8 for electron scales. ES and EM results are denoted by red triangles and blue circles respectively.

The contribution to the equilibrium **ExB** shearing rate, $\omega_{se}$, from the ion pressure gradient has been estimated to be ~20% of the maximum growth rates for the ITG instabilities on the surfaces in this equilibrium. Including equilibrium rotational shear is likely to increase the shearing rate further, so that the ITG instabilities could be largely stabilised by sheared flows. Approximate mixing length estimates of transport coefficients, using $\chi \sim (\gamma_{max} - \omega_{se})/k_{max}^2$, suggest that ITG instabilities could give rise to thermal diffusivities of the order of 3-5 $m^2s^{-1}$ but that these transport coefficients will be sensitive to $\omega_{se}$ which could stabilise ITG modes. Mixing length arguments predict extremely weak transport coefficients arising from ETG instabilities, but these modes will not be stabilised by equilibrium sheared flows in this discharge owing to their large linear growth rates. The first nonlinear calculations of ETG turbulence [8] have found anomalous transport considerably in excess of mixing length estimates, and this was due to the existence of stable radially elongated

'streamer' structures, which are weakly damped by zonal flows.

**Discussion of Related Issues**

Fully nonlinear 5-D gyrokinetic calculations are required to obtain turbulent transport fluxes, and such calculations are extremely challenging due to the wide range of scales in length and time that have to be simulated. Progress on nonlinear calculations to study ETG turbulence in MAST and at high β in STs, is presented in [9], using GS2 on the EPSRC HPCx supercomputer in Daresbury.

Economic fusion power generation in the ST will require good confinement and stability in high β plasmas. Therefore it is crucial to develop our understanding of microinstability and turbulence properties in higher β plasmas, and this is discussed further in references [9,10]. Reference [11] presents microstability calculations for the plasma conditions envisaged for a conceptual design of high β ST power plant. While electrostatic modes were stabilised by β effects, modes with tearing parity were driven unstable on including electromagnetic effects. These tearing parity modes could be important for plasma performance in future ST devices. Reference [12] gives a more detailed discussion of the analysis presented in this paper.

**References**

[1] C M Roach et al, Nucl Fusion, **41**, 11, (2001).

[2] R J Akers et al, Nucl Fusion, **45**, A175, (2003).

[3] E J Synakowski et al, Plasma Phys Control Fusion, **44**, A165, (2002).

[4] M H Redi et al, 30th EPS Conf. on Contr. Fusion and Plasma Phys, St Petersburg 2003

[5] C Bourdelle et al, 7th ST Workshop, Sao Jose Dos Campos, Brazil, (2001).

[6] H Meyer et al, Plasma Phys Control Fusion, **46**, A291, (2004) and A R Field et al, 31st EPS Conf. on Contr. Fusion and Plasma Phys, London, (2004)

[7] M Kotschenreuther, G Rewoldt and W M Tang, Comp Phys Comm, **88**, 128, (1995).

[8] W Dorland et al, Phys Rev Lett, **85**, 5579, (2000).

[9] N Joiner et al, 31st EPS Conf. on Contr. Fusion and Plasma Phys, London, (2004).

[10] C Bourdelle et al, Phys Plasmas, **10**, 2881, (2003).

[11] H R Wilson et al, Nucl Fusion, (2004).

[12] D Applegate et al, submitted to Phys Plasmas (2004).

**Acknowledgements**

This work was funded jointly by the United Kingdom Engineering and Physical Sciences Research Council and by EURATOM. The authors are grateful to Clarisse Bourdelle, Jack Connor, Jim Hastie and Howard Wilson for useful discussions, and to Peter Knight and Terry Martin for helping with computational issues.